Korean J. Chem. Eng., **28**(7), 1511-1517 (2011)
DOI: 10.1007/s11814-011-0018-4

Intrinsic kinetics of one-step dimethyl ether synthesis from hydrogen-rich synthesis gas over bi-functional catalyst

Chengyuan Cheng, Haitao Zhang, Weiyong Ying†, and Dingye Fang

State Key Laboratory of Chemical Engineering, Engineering Research Center of Large Scale Reactor Engineering and Technology, Ministry of Education, East China University of Science and Technology, Shanghai 200237, China
(*Received 16 October 2010 • accepted 20 January 2011*)

Abstract−The reaction kinetics of the dimethyl ether synthesis from hydrogen-rich synthesis gas over bi-functional catalyst was investigated using an isothermal integral reactor at 220-260 ºC temperature, 3-7 MPa pressure, and 1,000-2,500 mL/g·h space velocity. The H_2/CO ratio of the synthetic gas was chosen between 3 : 1 and 6 : 1. The bi-functional catalyst was prepared by physically mixing commercial $CuO/ZnO/Al_2O_3$ and γ-alumina, which act as methanol synthesis catalyst and dehydration catalyst, respectively. The three reactions, including methanol synthesis from CO and CO_2 as well as methanol dehydration, were chosen as independent reactions. The Langmuir-Hinshelwood kinetic models for dimethyl ether synthesis were adopted. Kinetics parameters were obtained using the Levenberg-Marquardt mathematical method. The model was reliable according to statistical and residual error analyses. The effects of different process conditions on the reactor performance were also investigated.

Key words: Kinetics, Dimethyl Ether, Syngas, One-step, Fixed-bed

INTRODUCTION

Dimethyl ether (DME) is an important chemical intermediate for creating widely used chemicals, such as dimethyl sulfate, methyl acetate, and light olefins. It is also used as a substitute for liquefied petroleum gas [1]. It can be produced from a variety of feed-stock, such as natural gas, crude and residual oils, coal, waste products, and bio-mass. Numerous investigations have been carried out on DME to determine its suitability for use as a fuel in diesel-cycle engines [2]. Compared to some of the other leading alternative fuel candidates (i.e., methane, methanol, ethanol, and Fischer-Tropsch fuels), DME appears to have the largest potential impact on society and should be considered as the fuel of choice for eliminating the dependency on petroleum.

At present, DME is commercially prepared through dehydration of methanol using acidic porous catalysts, such as zeolites, silica-alumina, and alumina. Recently, an original technique called synthesis gas (syngas) to dimethyl ether (STD) process was developed for the direct synthesis of DME from synthesis gas in a single reactor with bi-functional catalysts composed of copper-based methanol synthesis and dehydration catalysts [3,4].

The main reactions in the STD process can be shown as follows:

Methanol synthesis:

$$CO+2H_2 \Leftrightarrow CH_3OH \quad \Delta H^0_{298\,K}=-90.7\ \text{kJ/mol} \tag{1}$$

$$CO_2+3H_2 \Leftrightarrow CH_3OH+H_2O \quad \Delta H^0_{298\,K}=-49.5\ \text{kJ/mol} \tag{2}$$

Methanol dehydration:

$$2CH_3OH \Leftrightarrow CH_3OCH+H_2O \quad \Delta H^0_{298\,K}=-23.5\ \text{kJ/mol} \tag{3}$$

Water gas shift (WGS):

$$CO+H_2O \Leftrightarrow H_2+CO_2 \quad \Delta H^0_{298\,K}=-41.2\ \text{kJ/mol} \tag{4}$$

Methanol is converted to DME through the dehydration of methanol (Eq. (3)) over an acid catalyst. Then, the equilibrium conversion shifts towards the right-hand side of the methanol synthesis reaction (Eqs. (1) and (2)). The combination of these reactions results in a synergistic effect, relieving the unfavorable thermodynamics for methanol synthesis: methanol, which is produced in the first two reactions, is consumed to produce DME and water. Water and carbon monoxide are converted in the WGS reaction (Eq. (4)) into carbon dioxide and hydrogen, the latter being a reactant for the methanol synthesis. Thus, one of the products in each step is a reactant for another one. This creates a strong driving force for the overall reaction, allowing for a very high synthetic gas conversion in one single pass.

At present, research on direct DME synthesis is focused on catalyst and process. However, to provide basic data for designing a reactor for a plant or industry, the kinetics study of direct DME synthesis is necessary. The establishment of an industry-scale slurry reactor has not been reported so far due to the scarcity of experience in reactor scaling up. The vast amount of information available on the design and operation of the fixed-bed reactor allows for its easy and rapid construction on an industrial scale.

In a fixed-bed reactor, the chief difficulty would be the prevention of the occurrence of hot spots, since the reactions involved in the synthesis of DME are highly exothermic. Compared to the process of DME synthesis from CO-rich syngas, the process of DME synthesis from hydrogen-rich syngas has less heat release and high CO conversion. So the hydrogen-rich CO-lean syngas is best suited for DME synthesis in the fixed-bed reactor [5]. Whereas, in the industry process the outlet reactant gas which was not reacted will recycle into the inlet of the reactor, and mix with the fresh gas. So

†To whom correspondence should be addressed.
E-mail: wying@ecust.edu.cn

the real concentration of the reactant gas reacted in the catalyst bed was hydrogen-rich CO-lean syngas. Thus, it is necessary to investigate the kinetics of DME synthesis using syngas, which is rich in hydrogen.

The kinetics of DME synthesis from syngas, which H_2/CO from 1 to 2, has been investigated in a large number of studies, but the kinetics of DME synthesis from hydrogen-rich CO-lean syngas has not been reported yet. In the present study, the intrinsic kinetics of one-step DME synthesis from hydrogen-rich syngas, which H_2/CO from 3 to 6, over the CuO-ZnO-Al_2O_3/γ-alumina catalyst in isothermal integral reactor is investigated. The kinetics model for this process, which could be used in fix-bed reactor design, is based on the Langmuir-Hinshelwood mechanism. Moreover, the influence of different process conditions, such as pressure, temperature, and space velocity, is simulated by the proposed kinetics model.

EXPERIMENTAL

1. Catalyst

The bi-functional catalyst (BFC) was prepared by admixing the two commercial catalysts: methanol synthesis catalyst, XNC-98, and methanol dehydration catalyst, CNM-3. Two commercial catalysts were finely milled and sieved to a size of less than 120 μm to avoid mass-transfer limitation and then mixed well at a mass ratio of 1 : 1. This mass ratio was obtained from a previous study [6]. The BET results including pore volume, pore average diameter and measured surface areas are shown in Table 1. The XRD patterns of three catalysts are shown in Fig. 1.

2. Experimental Set-up

Fig. 2 presents a schematic view of the fixed-bed reactor set-up that was used for the acquisition of the kinetics data. The STD reaction kinetics study was carried out in an isothermal integral reactor (Φ24 mm×6 mm×600 mm), which contained 6.005 g catalyst. The catalyst was mixed well with quartz wool of the same size. The top and bottom of the catalyst bed were also filled with quartz wool to ensure that $L/d_r>8$. Since the reactor diameter was 18 mm and the pellet size never surpassed 0.8 mm, the ratio d_r/d_p always exceeded 22, ensuring a uniform distribution of the feed over the reactor section [7]. The feed gas was deoxidized before entering the reactor. There was a backpressure regulator after the reactor. The down line effluent was kept at a constant temperature of over 100 °C to avoid possible condensation of water or methanol.

Before each kinetic test, the catalyst was activated in situ through reduction using a flow of 5% H_2 in N_2 at 240 °C approached at 1 °C/min from room temperature for 12 h. The catalyst was then cooled to the reaction temperature in the presence of hydrogen gas. After this pre-treatment, the feed (H_2 : CO : CO_2 : N_2) was introduced into the fixed-bed reactor. A small portion of the reactor effluent was sent to the gas chromatograph for on-line analysis. The thermal conductivity detector with a TDX-01 column in the gas chromatograph was used to analyze H_2, N_2, CO, CO_2, and CH_4 (Ar as the carrier

Table 1. The BET results

Sample	Pores volume (cm^3/g)	Pore average diameter (nm)	Surface area (m^2/g)
BFC	0.3430	8.36	164.1
XNC-98	0.2299	8.99	102.3
CNM-3	0.4799	8.08	237.4

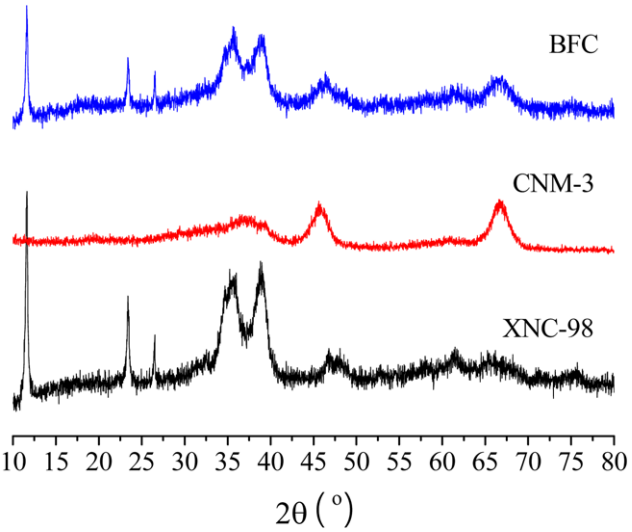

Fig. 1. XRD patterns of methanol synthesis catalyst (XNC-98), dehydration catalyst (CNM-3) and bi-functional catalyst (BFC).

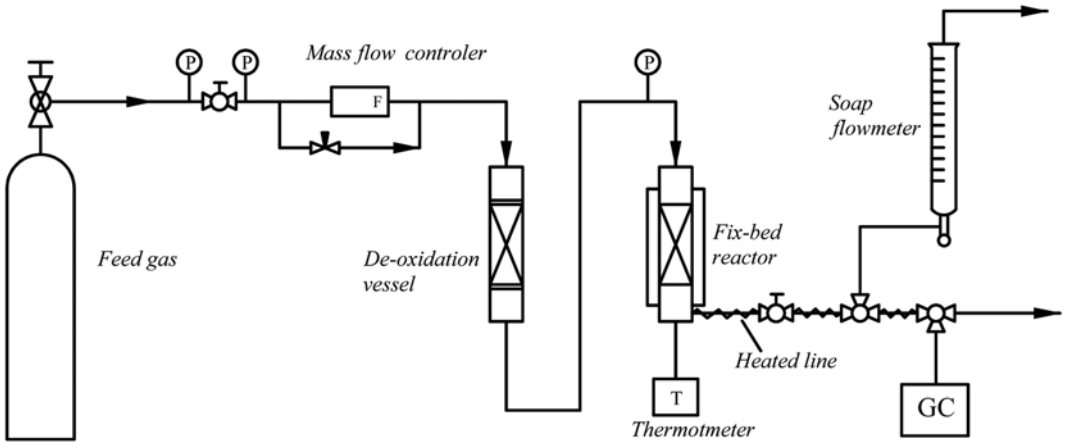

Fig. 2. Schematic view of the isothermal integral reactor system used in the kinetics data acquisition.

Table 2. Experimental data of the intrinsic kinetics of one-step DME synthesis from synthetic gas

No	t, °C	P, MPa	SV, mL/(g·h)	$y_{CO,\,in}$	$y_{CO2,\,in}$	$y_{H2,\,in}$	$y_{CO,\,out}$	$y_{CO2,\,out}$	$y_{DME,\,out}$
1	250.3	3.00	1500	0.1921	0.0488	0.6538	0.1434	0.1158	0.0721
2	250.1	3.05	1500	0.1262	0.0333	0.7331	0.0701	0.0853	0.0678
3	250.1	4.01	1500	0.1921	0.0488	0.6538	0.1106	0.1254	0.0949
4	250.1	4.05	1500	0.1262	0.0333	0.7331	0.0506	0.0847	0.0786
5	240.0	4.95	2000	0.1524	0.0174	0.6962	0.0449	0.0284	0.0596
6	250.1	4.95	2500	0.1262	0.0333	0.7331	0.0696	0.0699	0.0477
7	249.9	5.00	1000	0.1262	0.0333	0.7331	0.0185	0.0907	0.1169
8	250.0	5.00	1000	0.1921	0.0488	0.6538	0.0436	0.1510	0.1581
9	250.0	5.00	2000	0.1921	0.0488	0.6538	0.1258	0.1097	0.0732
10	250.0	5.00	2500	0.1921	0.0488	0.6538	0.1444	0.1003	0.0517
11	260.1	5.00	1500	0.1262	0.0333	0.7331	0.0338	0.0874	0.0935
12	250.0	5.01	2500	0.1524	0.0174	0.6962	0.0494	0.0246	0.0605
13	220.3	5.05	1500	0.1921	0.0488	0.6538	0.1411	0.0847	0.0461
14	220.4	5.05	1500	0.1262	0.0333	0.7331	0.0509	0.0563	0.0399
15	229.8	5.05	1500	0.1262	0.0333	0.7331	0.0454	0.0701	0.0528
16	229.9	5.05	1500	0.1921	0.0488	0.6538	0.1165	0.1000	0.0614
17	240.0	5.05	1500	0.1921	0.0488	0.6538	0.0973	0.1181	0.0840
18	240.1	5.05	1500	0.1262	0.0333	0.7331	0.0423	0.0794	0.0658
19	249.9	5.05	2000	0.1262	0.0333	0.7331	0.0568	0.0771	0.0646
20	260.0	5.05	1500	0.1921	0.0488	0.6538	0.0695	0.1404	0.1252
21	250.2	6.00	1500	0.1262	0.0333	0.7331	0.0317	0.0822	0.0925
22	249.9	6.02	1500	0.1921	0.0488	0.6538	0.0724	0.1281	0.1251
23	250.0	7.00	1500	0.1262	0.0333	0.7331	0.0258	0.0815	0.1045
24	250.3	7.00	1000	0.1524	0.0174	0.6962	0.0376	0.0195	0.0810
25	250.0	7.03	1500	0.1921	0.0488	0.6538	0.0603	0.1276	0.1492

gas). The flame ionization detector and HP-INNOWAX were used in the other gas chromatograph to analyze DME, methanol, CH_4, and other organic products (N_2 as the carrier gas).

3. Experimental Conditions

The kinetic experiments were performed under steady-state conditions. Mass and heat transfer limitations were negligible under the chosen experimental conditions. Both internal and external particle diffusion resistance were confirmed as absent.

To do kinetics modelling, a broad range of experimental conditions were carried out under the following reaction conditions: 220-260 °C, 3-7 MPa, 1,000-2,500 mL/g·h, which was sufficiently far from the equilibrium conditions. The reactant was mixed by H_2, N_2, CO, CO_2 at proper ratio, and the composition of reactant was H_2: 60-75%, N_2: 9-12%, CO: 12-20%, CO_2: 1-5%.

RESULTS

Twenty-five groups of experimental data were obtained under different reaction temperatures, pressure, and space velocities in the given experimental range. The results are listed in Table 2.

1. Simulation and Parameter Estimate

Several kinetics models for methanol synthesis and methanol dehydration reactions were tested under both methanol and DME synthetic conditions [8-12]. In the STD process, methanol was obtained from the synthesis of both CO and CO_2 [13]. To better understand the process, especially the relationship of CO and CO_2 synthesis to methanol, we conducted an intrinsic kinetic research and chose Eqs. (1), (2) and (3) as independent reactions. From the initial screening, the model for methanol synthesis from both CO and CO_2 and for methanol dehydration based on dual-site Langmuir-Hinshelwood mechanism were selected for the analysis and simulation of the combined process [14,15]. The intrinsic kinetics rate equations are as follows:

$$r_{CO}=-\frac{dN_{CO}}{dW}=\frac{k_1 f_{CO} f_{H_2}^2(1-f_M/K_{f1} f_{CO} f_{H_2}^2)}{(1+K_{CO} f_{CO}+K_{CO_2} f_{CO_2}+K_{H_2} f_{H_2})^3} \tag{5}$$

$$r_{CO_2}=-\frac{dN_{CO_2}}{dW}=\frac{k_2 f_{CO_2} f_{H_2}^3(1-f_M f_{H_2O}/K_{f2} f_{CO} f_{H_2}^3)}{(1+K_{CO} f_{CO}+K_{CO_2} f_{CO_2}+K_{H_2} f_{H_2})^4} \tag{6}$$

$$r_{DME}=\frac{dN_{DME}}{dW}=\frac{k_3 f_M(1-f_{DME} f_{H_2O}/K_{f3} f_M^2)}{(1+\sqrt{K_M f_M})^2} \tag{7}$$

The fugacity of each component was calculated with the SHBWR equation, where K_f is the equilibrium of the reaction [15,16]. CO, CO_2, and DME were chosen as the key components. The reaction rates of methanol synthesis from CO and CO_2 (Eqs. (5) and (6)), and the methanol dehydration to DME (Eq. (7)) are expressed as:

$$\frac{dy_{CO}}{dW}=\frac{-(1-2y_{CO}-2y_{CO_2})}{N_{in}(1-2y_{CO,in}-2y_{CO_2,in})^2}[(1-2y_{CO})r_{CO}-2y_{CO}r_{CO_2}] \tag{8}$$

$$\frac{dy_{CO_2}}{dW}=\frac{-(1-2y_{CO}-2y_{CO_2})}{N_{in}(1-2y_{CO,in}-2y_{CO_2,in})^2}[(1-2y_{CO_2})r_{CO_2}-2y_{CO_2}r_{CO}] \tag{9}$$

$$\frac{dy_{DME}}{dW}=\frac{(1-2y_{CO}-2y_{CO_2})}{N_{in}(1-2y_{CO,in}-2y_{CO_2,in})^2}[2y_{DME}(r_{CO}+r_{CO_2})-r_{DME}] \tag{10}$$

Table 3. Kinetic parameters for DME synthesis

Parameters	Pre-exponential factor	Activation energy (E), kJ/mol	Heat of adsorption (ΔH), kJ/mol
k_1	1.604×10^6	49,382	
k_2	3.465×10^3	40,526	
k_3	2.524×10^5	52,375	
K_{CO}	0.1357		804
K_{CO_2}	7.8261		1,134
K_{H_2}	0.0057		23,374
K_M	31.2208		528

The outlet concentration of the component was calculated using the Runge-Kutta method [17]. Parameter estimation was based on the minimization of the objective function:

$$S=\sum_{j=1}^{M}[\omega_{CO}(y_{CO,e,j}-y_{CO,c,j})^2+\omega_{CO_2}(y_{CO_2,e,j}-y_{CO_2,c,j})^2 + \omega_{DME}(y_{DME,e,j}-y_{DME,c,j})^2] \quad (11)$$

The Levenberg-Marquardt method [18] was used to determine the parameters of the kinetics models.

RESULTS AND DISCUSSION

1. Kinetics Parameters

To establish the kinetic parameters as a function of temperature, the following equation form was used: $k_i(T)=k_0\exp(-(E_i/RT))$, $K_i(T)=K_0\exp(\Delta H_i/RT)$, where $k_0(K_0)$ is the pre-exponential factor, E represents activation energy, and ΔH represents heat of adsorption (ΔH). The parameters of the proposed kinetics models are given in Table 3.

2. Statistical Analysis and Residual Error Analysis

ρ^2 is a coefficient of determination. It is calculated using the following formula:

$$\rho^2=1-\frac{\sum_{j=1}^{M}(y_{e,j}-y_{c,j})^2}{\sum_{j=1}^{M}y_{e,j}^2} \quad (12)$$

F is the rate of the sum of mean square to the sum of the mean square of the residual:

$$F=\frac{\left[\sum_{j=1}^{M}y_{e,j}^2-\sum_{j=1}^{M}(y_{e,j}-y_{c,j})^2\right]/Mp}{\sum_{j=1}^{M}(y_{e,j}-y_{c,j})^2/(M-Mp)} \quad (13)$$

where M is number of the experiments and Mp is number of parameters in the equation of the model.

Table 4 shows that the results of the statistical significance test of the parameters of the obtained model were reliable because $\rho^2>0.99$ and $F>10F_{0.05}$. $F_{0.05}$ is a value of F Table corresponding to 95% confidence level. If $\rho^2>0.9$ and $F>10F_{0.05}$, then the model is reliable.

Fig. 3-5 provide the comparison between the model prediction and the observed response data using the parameter estimation. It is clear that the dynamic model can provide a rough description of the trends in the transient responses.

Table 4. Statistics of the kinetics model

Equation	Mp	M-Mp	ρ^2	F	$10\times F_{0.05}$
(Eq. (1)) r_{CO}	8	17	0.9918	257.22	25.5
(Eq. (2)) r_{CO_2}	8	17	0.9929	509.35	25.5
(Eq. (3)) r_{DME}	4	21	0.9912	539.75	28.4

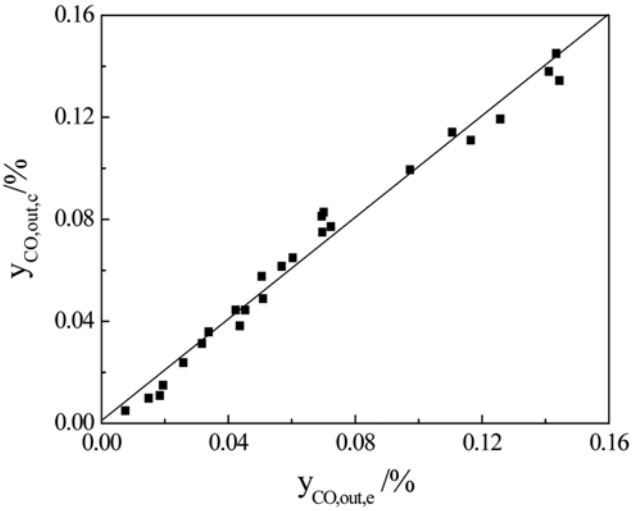

Fig. 3. Comparison of experimental data of CO mole fraction with the simulated results.

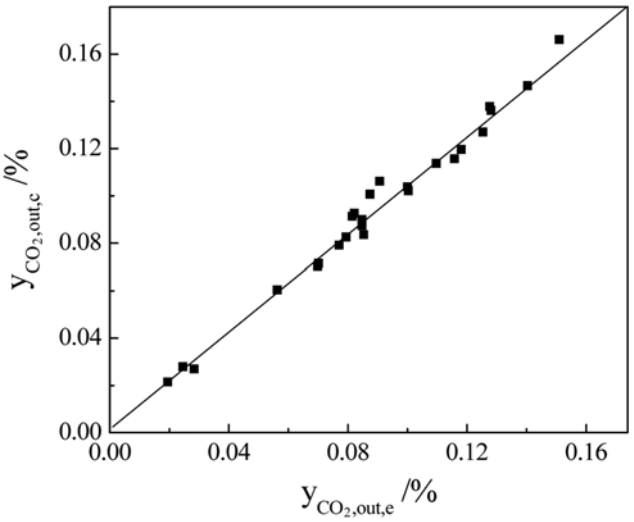

Fig. 4. Comparison of experimental data of CO_2 mole fraction with the simulated results.

We explored the dependence of the kinetics of DME synthesis on the operating conditions, such as temperature, pressure, and space velocity. For purposes of quantitative comparison with the experimental results, the conversion of the feed carbon monoxide and the yield of DME were used. These were defined as follows:

$$X_{CO}=\frac{N_{in}y_{CO,in}-N_{out}y_{CO,out}}{N_{in}y_{CO,in}} \quad (14)$$

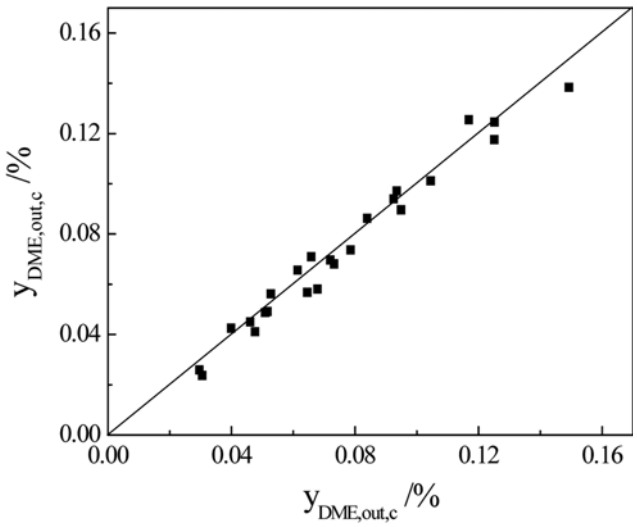

Fig. 5. Comparison of experimental data of DME mole fraction with the simulated results.

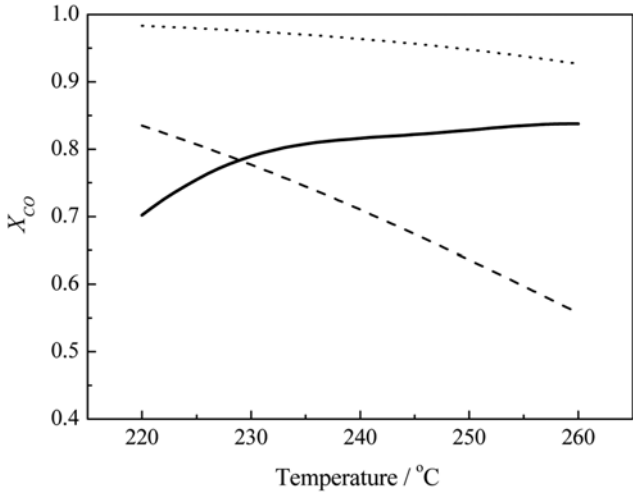

Fig. 6. Effect of temperature on the calculated conversion and equilibrium conversion of CO. Solid line: calculated conversion of CO, Dashed line: equilibrium conversion of CO in methanol synthesis reaction, Dotted line: equilibrium conversion of CO in DME synthesis reaction.

$$Y_{DME} = \frac{2 \times N_{out} y_{DME,out}}{N_{in} y_{CO,in} - N_{out} y_{CO,out}} \quad (15)$$

3. Synergy Effect in DME Synthesis Reactions

Fig. 6 shows the calculated conversion and equilibrium conversion of CO in both methanol synthesis and DME synthesis reaction. The equilibrium conversion in DME synthesis reaction is much higher than in methanol synthesis reaction. When the temperature is over 230 °C, the calculated conversion in DME synthesis reaction is higher than equilibrium conversion in methanol synthesis reaction, which certified that the advantage of synergistic effect in DME synthesis reaction is alleviation of the equilibrium limitation of methanol synthesis.

4. Effect of Temperature

Fig. 7 shows the influence of temperature on the conversion of CO. As is observed, when temperature was increased in the range of 220 to 260 °C, the conversion of CO increased because the reaction rate was kinetically controlled in this region. The equilibrium conversion of CO decreased as the temperature rose, so the reaction was controlled by a shift in the thermodynamic equilibrium at high temperatures, and the thermodynamic influence became dominant in such a case. Since methanol synthesis and methanol dehydration were both exothermic reactions, a higher temperature led to an unfavorable effect on the equilibrium conversion of synthesis gas.

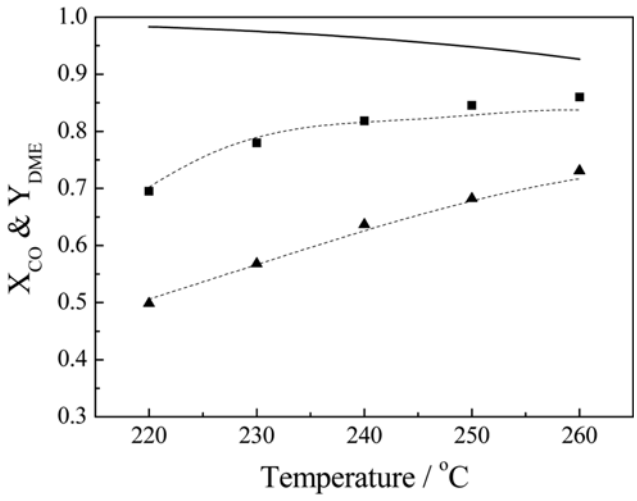

Fig. 7. Effects of temperature on the simulation and experimental results: P=5 MPa, SV=1,500 mL/g·h (■) CO conversion, (▲) DME yield; Symbols: experimental, Dashed line: calculated. Solid line: equilibrium conversion of CO.

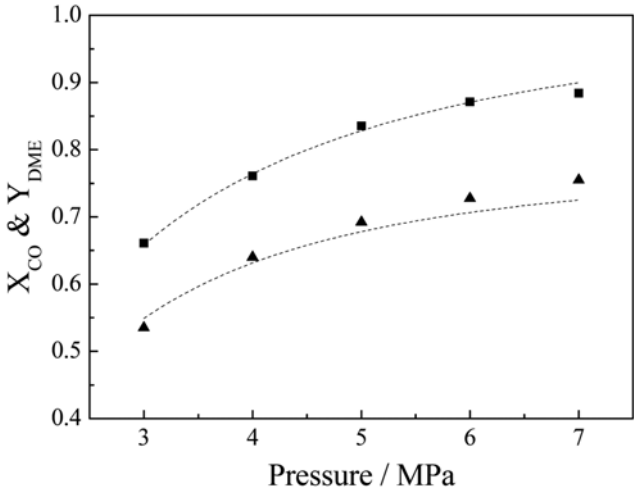

Fig. 8. Effect of pressure on the simulation and experimental results: t=240 °C, SV=1,500 mL/g·h. (■) CO conversion, (▲) DME yield; Symbols: experimental, Line: calculated.

5. Effect of Pressure

Fig. 8 shows the CO conversion as a function of the reaction pressure. The CO conversion increased when pressure was increased in the range of 3 to 7 MPa, which was the logical consequence of methanol synthesis as the limiting step of the whole reaction. Methanol synthesis was also a mole-number-reducing reaction, such that increased pressure favored the conversion of CO and DME yield.

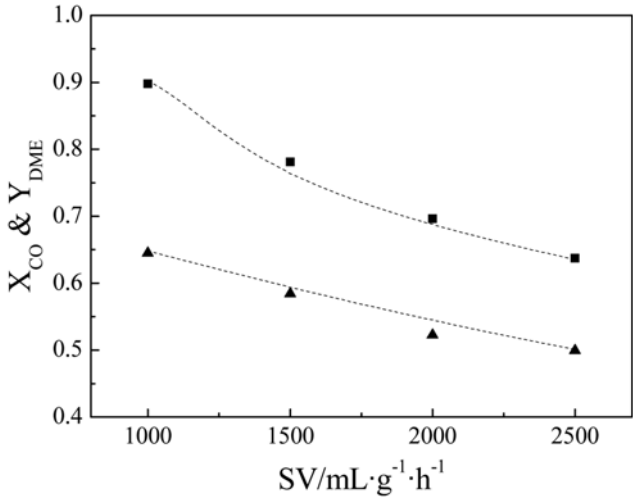

Fig. 9. Effect of space velocity on the simulation and experiment results: t=240 °C, P=5 MPa. (■) CO conversion, (▲) DME yield; Symbols: experimental, Line: calculated.

Since the number of moles on both sides of the methanol dehydration and water-gas shift reactions are the same, the pressure had no effect on these reactions. This implies that the reaction of DME production might be carried out under a pressure similar to the conversional synthesis of methanol.

6. Effect of Space Velocity

Fig. 9 shows the effect of space velocity on the performance of STD. The CO conversion and DME yield decreased with the increase in space velocity. A higher space velocity means shorter residence time of reactants in contact with the catalyst, and a short residence time was unfavorable for the consecutive reactions. The DME yield did not decrease as much as the CO conversion.

CONCLUSIONS

An intrinsic kinetics model for the DME synthesis from synthetic gas with rich hydrogen was established in terms of the Langmuir-Hinshelwood mechanism. Methanol synthesis from CO and H_2 and from CO_2 and H_2 and the methanol dehydration were chosen as three independent reactions. The experiments used to determine the kinetic parameters were performed with industrial CuO-ZnO-Al_2O_3/γ-alumina catalysts under the following conditions: pressures between 3 and 7 MPa, temperatures varying between 220 and 260 °C, and space velocities between 1,000 and 2,500 mL/g·h. The simulation data agreed well with the experimental results over a wide range of experimental conditions. This accurate kinetics model can be used in potential reactor modelling and scaling-up of a fixed-bed reactor. Furthermore, the kinetics equations described the influence of temperature, pressure, and space velocity in a physically acceptable manner. The STD process was favorable at high temperatures, pressure, and low space velocity.

ACKNOWLEDGEMENTS

The authors gratefully acknowledge the financial support by the National Technology Support Program of China (2006BAE02B02), and by National Basic Research Program of China (2005CB221205).

NOMENCLATURE

d_r : diameter of reactor [mm]
d_p : diameter of catalyst particle [mm]
f : fugacity [MPa]
k : reaction rate constants
K : adsorption constants
L : length of catalyst bed [m]
N : molar flow rate [mol/h]
P : pressure [MPa]
r : rate of reaction [mol/(g·h)]
t : temperature [°C]
T : temperature [K]
X : conversion [%]
y : mole fraction of components [%]
Y : yield [t/d]
W : weight of catalyst [g]
ΔH : the heat of reaction [kJ/mol]
ω : weight factor

Subscript

c : calculated result
e : experiment result
in : inlet of the reactor
out : outlet of the reactor
M : methanol

REFERENCES

1. T. A. Semelsberger, R. L. Borup and H. L. Greene, *J. Power Sources*, **156**, 497 (2005).
2. C. Arcoumanis, C. Bae and R. Crookes, *Fuel*, **87**, 1014 (2008).
3. D. M. Brown, B. L. Bhatt, T. H. Hsiung, J. J. Lewnard and F. J. Waller, *Catal. Today*, **8**, 279 (1991).
4. J. C. Xia, D. S. Mao, B. Zhang, Q. L. Chen and Y. Tang, *Catal. Lett.*, **98**, 235 (2004).
5. W. Z. Lu, L. H. Teng and W. D. Xiao, *Natural Gas Chem. Ind. (China)*, **27**, 53 (2002).
6. D. H. Liu, J. Xu, H. T. Zhang and D. Y. Fang, *J. Chem. Ind. Eng. (China)*, **53**, 103 (2002).
7. G. F. Froment and K. B. Bischoff, *Chemical reactor analysis and design*, Wiley, New York (1990).
8. K. L. Ng, D. Chadwic and B. A. Tosland, *Chem. Eng. Sci.*, **54**, 3587 (1999).
9. G. Bercic and J. Levec, *Ind. Eng. Chem. Res.*, **31**, 399 (1992).
10. K. M. Vanden Bussche and G. F. Froment, *J. Catal.*, **161**, 1 (1996).
11. G. H. Graaf, E. J. Stamhuis and A. A. C. M. Beenackers, *Chem. Eng. Sci.*, **43**, 3185 (1988).
12. G. R. Moradi, J. Ahmadpour and F. Yaripour, *Chem. Eng. J.*, **144**, 88 (2008).
13. J. S. Lee, K. H. Lee, S. Y. Lee and Y. J. Kim, *J. Catal.*, **144**, 414 (1993).
14. W. D. Song, B. C. Zhu and H. S. Wang, *J. Chem. Ind. Eng. (China)*, **38**, 401 (1988).
15. Z. G. Nie, H. W. Liu, D. H. Liu, W. Y. Ying and D. Y. Fang, *J. Nat.*

Gas. Chem., **14**, 22 (2005).
16. H. T. Zhang, F. H. Cao, D. H. Liu and D. Y. Fang, *Journal of East China University of Science and Technology*, **27**, 198 (2001).
17. R. W. Hamming, *Numerical methods for scientists and engineers*, Dover, New York (1983).
18. S. Roweis, Levenberg-Marquardt Optimization University of Toronto (1996).